MAX-PLANCK-INSTITUT
FÜR PLASMAPHYSIK

IPP-Report

G. Pautasso, A. Herrmann and ASDEX Upgrade Team

Power Load on the ASDEX Upgrade Divertor during Disruptions: a Portfolio

IPP 2024-27
Oktober 2024

IPP Report

Power Load on the ASDEX Upgrade Divertor during Disruptions: a Portfolio

G. Pautasso, A. Herrmann and ASDEX Upgrade Team

11 October 2024

Content

- Introduction

- G. Pautasso et al., *Energy balance during disruption associated with vertical displacement events*, published in Nucl. Fusion (1994) 34 455

- G. Pautasso et al., *Analysis of the power deposition in the ASDEX Upgrade divertor during disruptions,*
(4 pages contribution and poster) 30th EPS Conference on Contr. Fusion and Plasma Phys., St. Petersburg, 7-11 July 2003 ECA Vol. 27A, P-1.135

- G. Pautasso et al., *Details of power deposition in the thermal quench of ASDEX Upgrade disruptions,*
(4 pages contribution and poster) 31st EPS Conference on Contr. Fusion and Plasma Phys., London, 28 June - 2 July 2004 ECA Vol.28G, P-4.132

Introduction

The deposition of energy on the plasma facing components, PFCs, of a tokamak during a disruption is a problem of concern for future fusion reactors of the tokamak type. The problem was extensively reviewed and discussed in Chapter 3 of the ITER Physics Basis review paper [1] and in the follow-up paper “Progress in the ITER Physics Basis” [2]. Since then, little progress has been made to reduce or even eliminate the uncertainties, which affect the extrapolation of an unmitigated heat flux onto PFCs during the thermal and the current quench to devices different from and/or larger than the existing ones.
Most of the work done in this area at present tokamaks and at ASDEX Upgrade preceded the publication of [2]. The documentation and analysis of the heat load on the JET Be-W wall continued also afterwards, because of the relevance of JET in the stepladder to a fusion reactor and because of minor melting events observed in the device.
ASDEX Upgrade – on its part - contributed significantly with thorough analyses of experimental measurements to both [1] and [2]. The tokamak has been equipped with infra-red (IR) cameras and bolometers since the beginning of its operation. Moreover, the coverage of the IR diagnostic was best (for the purpose of studying power loads onto the divertor during disruptions) in the first decade of operation. The work of analysis done in that period was presented at ITER Expert Group Meetings, in workshops and in conferences. In the following years, the IR diagnostic was almost exclusively set up to study ELMs and heat fluxes onto the divertors during the plasma discharge but not during disruptions.

The unknowns encountered when extrapolating the heat fluxes to new tokamaks have not been resolved for several reasons:

- the measurements needed are problematic because spatial coverage and/or time resolution are insufficient, spurious effects affect the measurements (e.g. plasma radiation in addition to IR radiation), the measurements are saturated, appropriate diagnostics are unavailable;
- the experiments have not been a priority in the experimental campaigns, although dedicated plasma conditions are often needed;
- simulations have been difficult up to now because they require the use of non-linear MHD codes, which are not yet always able to reproduce the evolution of the magnetic field during the thermal and the current quench.

The main unknown in the extrapolation problem is the extent of the heat flux deposition surface. The heat flux onto a surface of area S can be written as $h \propto E_{th} f_{as} / \left(S \sqrt{\tau_{TQ}}\right)$
where E_{th} is the thermal energy content of the plasma, τ_{TQ} is the thermal quench time alias the duration of the heat pulse and f_{as} is an asymmetry factor.

- The maximum energy content of a fusion reactor being designed can be assumed known, since the scaling of confinement time and the magnitude of the input power are design parameters. Typically the thermal energy at the thermal quench is degraded with respect to the maximum thermal energy, which reduces the maximum thermal load calculated assuming good confinement.
- There are scaling laws for the thermal quench time and physics justifications for its magnitude and scaling.
- The asymmetry factor due to MHD events is not known but could be studied with appropriate numerical codes and validated with appropriate measurements
- Misaligned tiles – impossible to predict - and their edges can intercept magnetic surfaces with an up-to 90 degree angle and are subject to large localized heat fluxes.

- There are huge discrepancies in what the deposition surface is believed to be: In JET the plasma thermal energy was never found to be completely deposited in the divertor, that hints to a deposition surface larger than the divertor; in ASDEX Upgrade the plasma thermal energy was typically found to be deposited on the large divertor plate surface; in TEXTOR the broadening of the e-folding length of the deposition was twice the same quantity during the discharge.

We often observe that the slow pace at which fusion is developing and the lack of rigor in reviewing relevant past work cause the loss of already-acquired valuable knowledge. For these reasons, the authors decided to make available these old works now in the form of an IPP report. Complementary work on mitigated heat loads can be found in [3]-[5].

Acknowledges.
Many thanks to M. Maraschek, who helped us recover old IslandDraw figures and transform them in .eps and other usable file formats.

References

[1] ITER Physics Expert Group on Disruptions, Plasma Control, and MHD and ITER Physics Basis Editors 1999 Chapter 3: MHD stability, operational limits and disruptions Nucl. Fusion 39 2251
[2] T.C. Hender et al 2007 Nucl. Fusion 47 S128
[3] G. Pautasso et al 1996 Nucl. Fusion **36** 1291
[4] G. Pautasso et al., Fusion Science and Technology, Vol. 44, Nov. 2003, p. 716-729
[5] G. Pautasso et al., Plasma Physics and Controlled Fusion 59, 1 (2017) 014046

ENERGY BALANCE DURING DISRUPTION ASSOCIATED WITH VERTICAL DISPLACEMENT EVENTS

G. PAUTASSO, A. HERRMANN, K. LACKNER, ASDEX UPGRADE TEAM

(Max-Planck Institut fuer Plasmaphysik, Garching, Germany)

ABSTRACT.

The presence of an extended region of open flux surfaces (halo), during the current quench phase of the disruption of elongated plasmas, is supported by measurements of halo currents and by numerical simulations. The halo, in addition to providing a poloidal current path between the plasma and the first-wall components, allows rapid conduction and convection of energy along field lines, and therefore a mechanism for the localized deposition of energy onto the wall. The heat load to the region of the plasma-first-wall interaction is higher than in the scenario in which the magnetic energy is mostly dissipated by radiative processes.

1. INTRODUCTION

The spatial and temporal characterization of power deposition during disruption is necessary for the design of the plasma facing components in ITER [l]. Particularly in a tokamak with an elongated cross-section, disruptions and loss of position control are closely related, so that ASDEX Upgrade, with its distant shaping coils, is especially suited for these studies. In addition, its diagnostic apparatus allows the plasma shape and energy to be reconstructed from magnetic measurements, the measurement of currents flowing between plasma and vessel components, and the monitoring of the heat load onto the divertor target plates by means of a high-time-resolution thermography system. The Tokamak Simulation Code (TSC) [2], among others, is used to interpret the experimental data and gain insight into the observed phenomena. The measurements reported here verify the standard assumption that, during the thermal quench phase, a dominant fraction of the plasma thermal energy is deposited onto the target plates within a few hundred microseconds. During the current decay phase of so-called vertical disruptions, on the other hand, they show that a significant fraction of the poloidal field energy dissipation proceeds along the open flux surfaces of the halo region, where the thermal contact along field lines to the target plates keeps the plasma temperature and hence the conductivity to a low value.
This scenario differs from the current decay phase of vertically well controlled limiter plasmas [3], for which the penetration of impurities across field lines and into the bulk plasma has to be invoked to explain the high plasma resistivity and high power losses.

2. EVOLUTION OF DISRUPTIONS

Disruptions can have different causes (attainment of density or q limit, impurity injection or current ramp) and involve a complex sequence of events [4]. One can identify three major phases in the evolution of a disruption (see Fig. 1). In the first phase (I), the current density profile develops slowly in the direction of increasing tearing mode instability. Successively (II), a rapid rearrangement of the magnetic topology causes a change in current profile and the rapid loss of thermal energy. In the last phase (III), the plasma current decays because of increased resistivity of the plasma column. Furthermore, the disruption of an elongated plasma is commonly accompanied by the loss of vertical stability due to changes in plasma impedance and in the mutual inductance between the plasma and the stabilizing system. During the vertical displacement of a disrupting

plasma, halo currents arise [5] and the evolution of the current quench phase becomes strongly dependent on the coupling between plasma and machine.
Time traces of a typical density limit disruption in ASDEX Upgrade [6] are shown in Fig. 1 (shot 2627, B = -1.35 T, I_p = 800 kA, single null). A minor disruption, which results in the expulsion of 40% of the electron density (n_e) and of the thermal energy (W_{th}), takes place at t = 2.13 s. The total radiated power (P_{rad}), as measured by the bolometer, increases further in the following few milliseconds, exceeding the ohmic power. The terminal disruption then starts with the current spike at t = 2.162 s; changes in the plasma impedance, also occurring at this time, cause the onset of the vertical displacement (z_{curr} is the vertical position of the plasma current centre).

3. POWER BALANCE DURING DISRUPTION

The thermography system installed on ASDEX Upgrade [7] is particularly suited for monitoring rapidly changing heat fluxes deposited on the divertor plates during disruptions. It scans the entire poloidal extension of the lower divertor plates, at one toroidal location, with a space resolution of 3.4 mm/pixel on the inner plate and 2.72 mm/pixel on the outer plate, and with a time resolution of more than 130 µs. Assuming toroidal symmetry of the divertor thermal load, we can assess the energy balance of the entire discharge. Figure 2 shows time traces of energy losses during the phase preceding the terminal disruption. The decrease of plasma density observed in Fig. 1, at t = 2.13 s is accompanied by a 50% decrease of the plasma thermal energy, which is mostly lost through the SOL to the divertor plates. In this phase we verify that

$$\left(\int_{t_0}^{t} P_{\mathrm{oh}}\,\mathrm{d}t - \Delta W_{\mathrm{th}}\right) \Big/ \int_{t_0}^{t} (P_{\mathrm{rad}} + P_{\mathrm{div}})\,\mathrm{d}t \simeq 1 \qquad (1)$$

where P_{oh} is the ohmic input power and $P_{div} = P_{div,in} + P_{div,out}$ is the sum of the power deposited onto the inner (in) and outer (out) bottom divertor plates.
During the terminal disruption the power deposition to the target plates shows a ragged temporal structure (Fig. 3). The first major peak coincides with the negative voltage spike (not shown) and the current rise. The power losses to the divertor plates integrated during the first peak duration account for the pre-disruption thermal energy of the plasma (~ 45 kJ). This is in agreement with the widely confirmed observation that, during the thermal quench, the electron temperature drops rapidly to values between 50 and 100 eV or lower [l] and that, during this process, the plasma loses most of its thermal energy. In addition, with a time resolution of 260 µs (the best used to the present time), we can assess that this process happens on a time-scale of several hundred microseconds. The poloidal profile shows that the power is broadly distributed on the plate surface. The radiated power is also increasing during this phase. With the present time resolution of the bolometer (10 ms), we cannot resolve the radiated energy during the thermal quench. The series of peaks that follows the thermal quench coincides with the current decay and the halo current phase. The energy deposited onto the divertor during these 10 ms is higher than that during the thermal quench and amounts to 30% of the pre-disruption 850 kJ). plasma magnetic energy ($W_{mag} = L\, I_p^2/2$ ~ 850 kJ). An estimate of the total radiated power is at present not available for plasmas that are not in the midplane.
Figure 3 also shows the temporal evolution of the total halo current that flows between the plasma and the divertor plates; these measurements are provided by poloidal arrays of resistors located between divertor tiles and divertor support at one toroidal location.
These currents are induced by the rapid change in toroidal flux inside the vessel during the fast vertical motion of the plasma and the plasma current decay phase. During disruptions in ASDEX Upgrade, we commonly observe that the time evolution of these currents (as shown in Fig. 3) is well correlated to the heat flux onto the divertor plates. This indicates that a significant fraction of the magnetic energy, which is ohmically dissipated during the halo phase, is conducted and

convected along field lines to the plates. As the plasma β is low during this phase, the plasma current has to flow along field lines. The plasma motion towards the target plates induces a poloidal component of the halo current, $I_{h(\theta)}$, which closes through the vessel structures. The toroidal component of the halo current is related to the poloidal component as $I_h(\phi) = \langle q \rangle_h I_h(\theta)$, where $\langle q \rangle_h$ is a current density weighted average of the safety factor in the halo region. These processes are self-consistently modelled with the TSC code which shows [8] that, during the halo phase, a large fraction of the plasma current flows in a region of open field lines which closes through the vessel conducting structures (see Fig. 4). Simplified one dimensional power balance considerations indicate that a temperature gradient of some tens of electronvolts along field lines would allow for the ohmic power generated in the plasma (which has a higher resistivity with respect to the structures) to be conducted to the divertor plates.

4. CONCLUSIONS

During the thermal quench, which lasts a few hundred microseconds, the plasma thermal energy is mostly deposited onto the divertor plates. The implementation of the nominally smallest time resolution for the thermography system, the operation of the bolometer with a smaller integration time, along with the use of auxiliary heating, will soon allow a proper resolution of the power deposition distribution during disruptions and a characterization of its parametric dependence. We have identified a new mechanism of power deposition during vertical disruption. In the halo phase, the toroidal plasma current flows partially along field lines that intersect the vessel structure. The plasma open flux surfaces allow a rapid parallel transport of particles and heat to the divertor plates; this causes the deposition of a large fraction of the plasma magnetic energy onto the area of localized plasma-structure interaction. The resultant heat load there is higher than in the scenario in which the magnetic energy is dissipated by radiative processes. These observations have significant implications for the ITER design. In a tokamak with a high inductance superconducting PF coil system, the quadrupole component of the shaping field cannot be ramped down during a disruption at the rate of the plasma current decay. During the current decay phase the plasma will therefore always become positionally unstable at a plasma current of the order $1/f$ times the pre-disruption value, where f is the vertical stability margin of the unperturbed configuration [5]. The mechanism described in this paper will then occur, leading to additional heat loads onto the target plates. To minimize these thermal loads and the electromechanical effects of disruptions, the design should therefore have the largest possible f limit, as is in fact realized in the last (EDA) version of the ITER design.

ACKNOWLEDGEMENTS. The authors acknowledge fruitful discussions with Drs J. Neuhauser and O. Gruber.

REFERENCES

[1] ITER PHYSICS, ITER Documentation Series No. 21, IAEA, Vienna (1991)
[2] JARDIN, S.C., et al., J. Comput. Phys. 66 (1986) 481.
[3] WARD, D.J., WESSON, J.A., Nucl. Fusion 32 (1992) 1117.
[4] WESSON, J.A., et al., Nucl. Fusion 29 (1989) 641.
[5] GRUBER, O., et al., Plasma Phys. Control. Fusion 35 Suppl. B (1993) 191.
[6] MERTENS, V., et al., in Controlled Fusion and Plasma Physics (Proc. 20th Eur. Conf. Lisbon, 1993), Vol. 17C, Part I, European Physical Society, Geneva (1993) 267.
[7] HERMANN, A., et al., ibid., Part 11, p. 567.
[8] PAUTASSO, G., et al., ibid., Part I, p. 199.

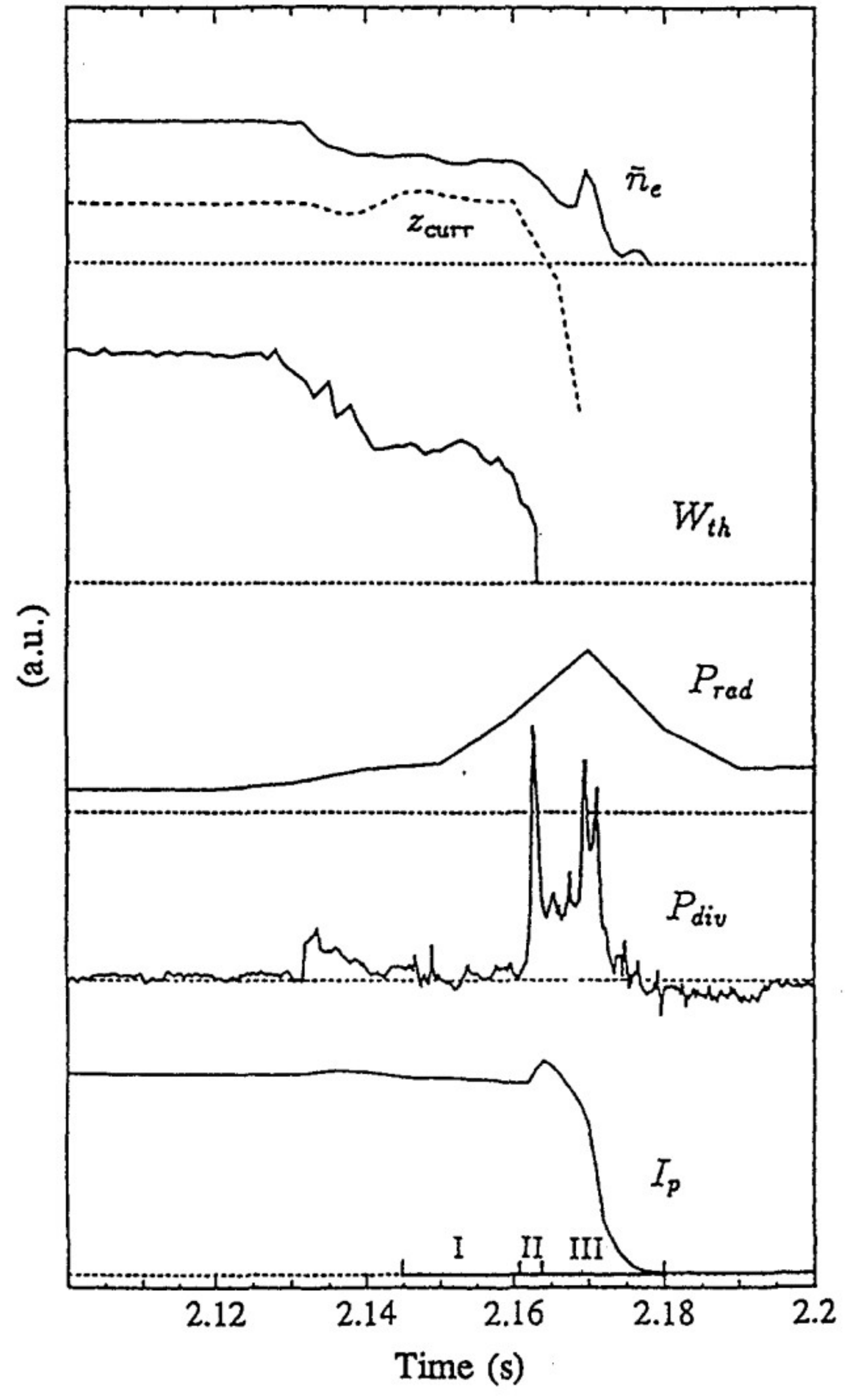

FIG. 1. Time evolution of plasma parameters that lead to a density limit disruption and loss of vertical control (n_e is the line average density; z_{curr} is the vertical position of the plasma current centre; W_{th} is the plasma thermal energy; P_{rad} is the radiated power; P_{div} is the power onto divertor plates; I_p is the plasma current).

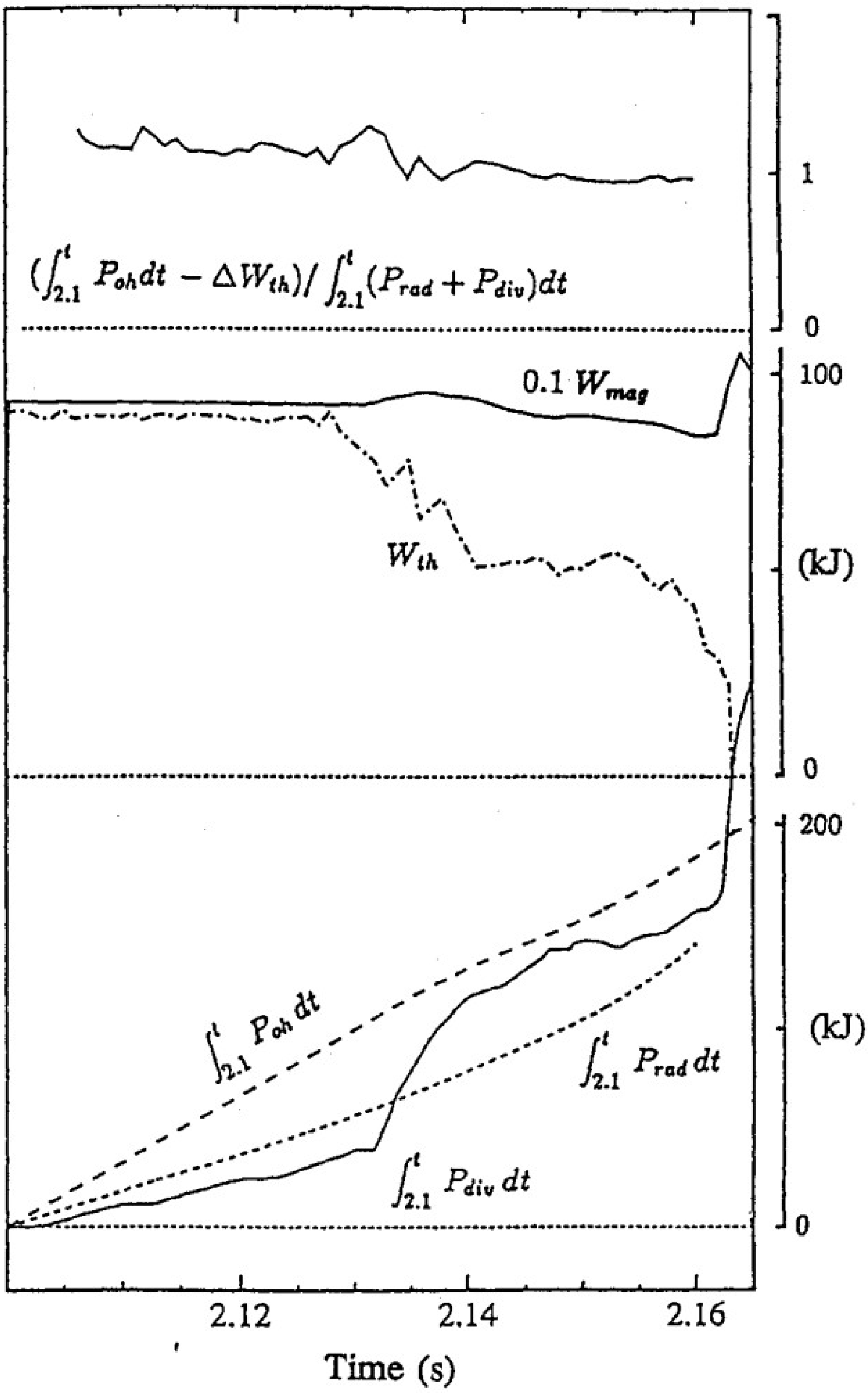

FIG. 2. Energy balance before terminal disruption: P_{oh}, P_{div} and P_{rad} are, respectively, ohmic, onto-divertor and radiated power; W_{th} and W_{mag} are the thermal and magnetic plasma energies.

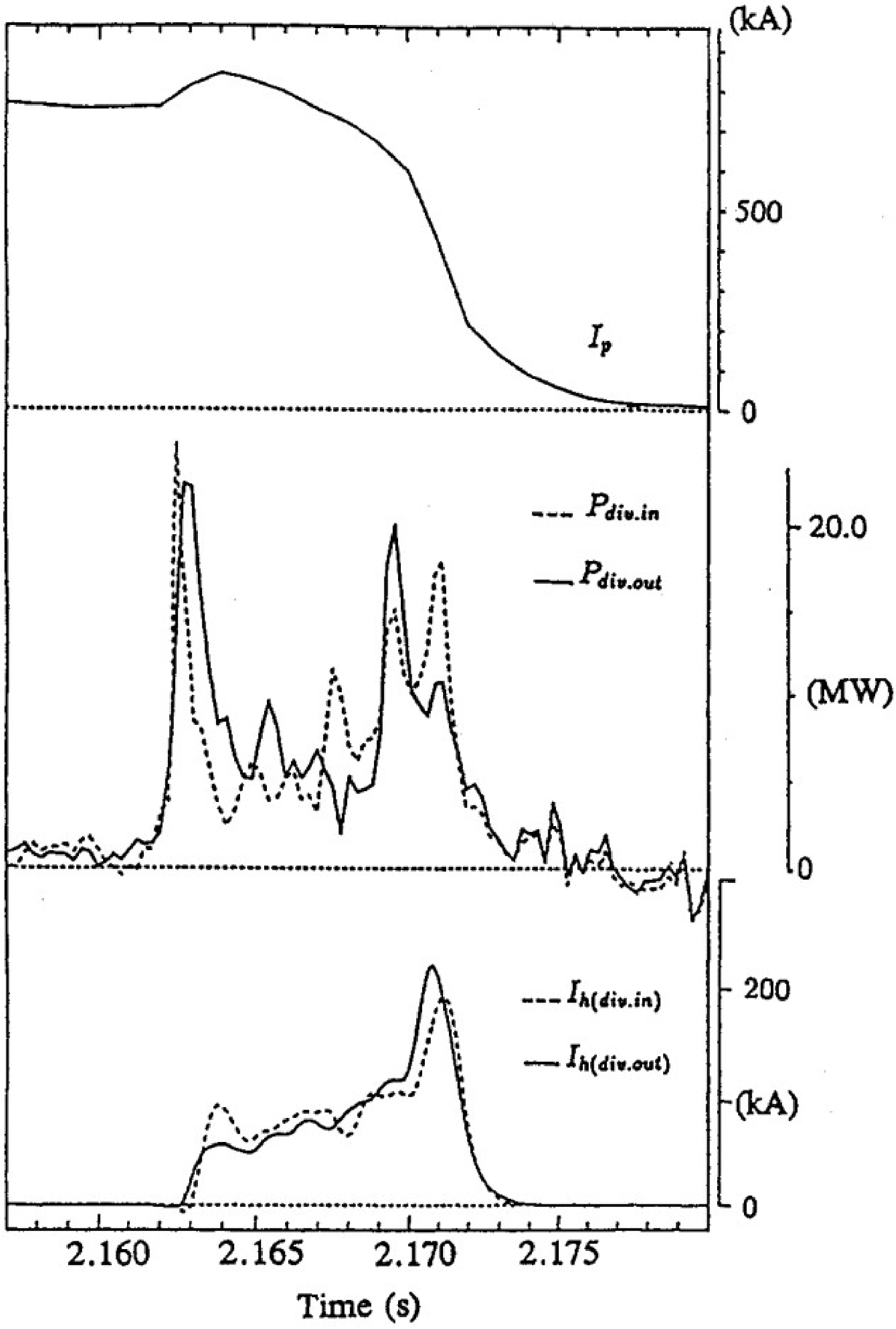

FIG. 3. Power flow (P_{div}) and halo currents (I_h) onto inner (*div.in*) and outer (*div.out*) divertor plates during the plasma current (I_p) decay phase.

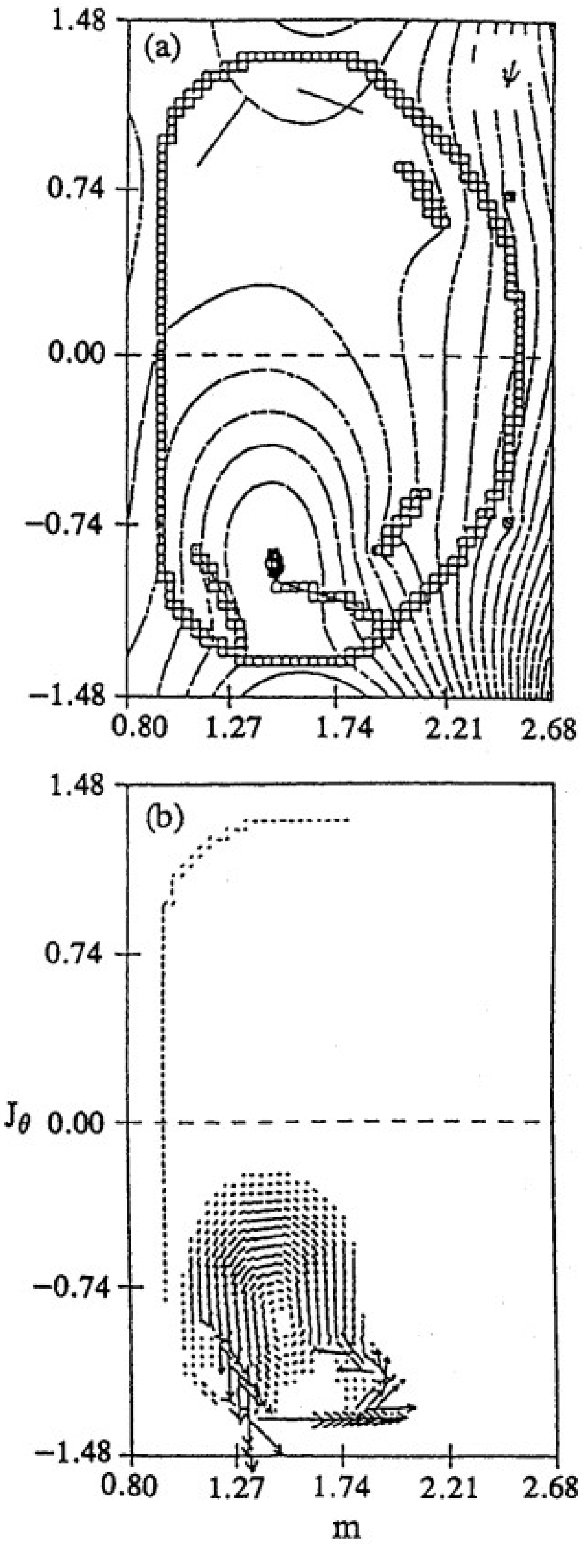

FIG. 4. TSC reconstruction of (a) poloidal flux surfaces (ψ) and (b) poloidal current distribution (J_θ) during current quench (I_p ~ *30%* $I_{p,\ nominal}$).

Analysis of the power deposition in the ASDEX Upgrade divertor during disruptions.

G. Pautasso, A. Herrmann, T. Eich, J.C. Fuchs, O. Gruber. A. Kallenbach and the ASDEX Upgrade Team, Max-Planck-Institut für Plasmaphysik, EURATOM Association, 85748 Garching, Germany

Introduction.

The power balance during disruptions in ASDEX Upgrade has been analized since the beginning of operation. The general picture of the power deposition mechanism in the Divertor I Phase (flat target plates) was as follows. The power density deposition profiles have always been so wide as to cover the whole divertor surface. During the thermal quench phase of the disruption up to 100 % of the thermal energy of the plasma was deposited onto the divertor plates within a few ms. In the successive current quench most of the magnetic energy associated with the plasma current was ohmically dissipated within the plasma and typically 30 % of it was found on the divertor plates. The majority of the disruptions in that experimental phase were density limits at relatively moderate plasma current (0.6-0.8 MA) and large q_{95} (4-6).

With the installation of the Divertor II-lyra and II-b and the exploration of new plasmas regimes (lower q_{95}, higher energy) the picture of power deposition has become more complex. In several discharges the thermal quench is relatively slow and the thermal energy starts leaking out of the plasma a few ms before the negative voltage spike. The power deposition profiles have remained very wide, spreading on the whole divertor surface and also outside of it (see Fig. 1).

Aim of this work is to check the power balance during recent disruptions and analyse the power deposition on the lower divertor plate from a statistical point of view.

Diagnostics.

Two IR thermography cameras, sensible to radiation with a 4.7 μm wavelength, measure the photon emission from the lower divertor plates. The power deposition profiles are then inferred from these raw data on the basis of a physical model. The two cameras are located at two different toroidal positions and observe not-overlapping poloidal regions of the divertor. The time resolution of the thermography data are in the range 0.12-1 ms; the spatial resolution is between 1 and 2 mm.

Radiation is measured by 100 bolometers mounted in 7 cameras around the plasma, which allow the reconstruction of the radiated power profile within and outside of the plasma separatrix. The time resolution of the bolometers is 1 ms.

The database.

The database, build for this work, contains 44 discharges (most of the disruptions) with complete measurements of the power deposition on the lower divertor plates in the shot range 13000-17500 (Jan.2000 - Mai.2003). The plasma parameters of the discharges varies in the following ranges: plasma current = 0.6-1 MA, q_{95} = 2.5-6, thermal energy before disruption = 50-500 kJ, magnetic energy 0.7-1.8 MJ, time interval between the thermal quench and the end of the current quench = 10-30 ms. The 30 discharges with number < 14200 pertain to the Divertor II-lyra configuration; the later 14 ones to the Diveror II-b geometry. The database contains disruptions with different causes; the differentiated discussion of the power balance for several disruption types is not yet aim of this paper.

Phenomenology.

The thermal energy of the plasma before disruption is in average much smaller (20 %) than the maximum thermal energy reached by the plasma during the discharge. The way the energy content of the plasma degrades before thermal quench varies: a large fraction of the energy may be lost during one or more minor disruptions, or it may continuously degrade within 10-100 ms.

The disruption consists of two phases: (1) the thermal quench, lasting a few ms, in which most of the plasma thermal energy is conducted along the scrape-off-layer to plasma facing components (wall or divertor); (2) the current quench, in which the electric current is dissipated by the enhanced resistivity of the cold plasma.

The energy may start leaking out of the plasma a few ms before thermal quench making the thermal quench itself a slow phenomenon lasting several ms. The parametric dependence of these different behaviors cannot be pointed out definitively yet. In any case the power deposition on the divertor plates during the thermal quench is not limited to a few 100s μs but lasts 2-3 ms in ASDEX Upgrade. The time of the thermal quench is chosen at the minimum (or center) of the negative voltage spike and has an accuracy of $\pm$ 0.5 ms.

By visual inspection of a large number of time histories of the spatially integrated power, we find that there is no one typical time history but a variety of them. The power density profiles are very broad and extend outside of the divertor region; details of the profile of energy deposition are discussed further in the paper.

Energy balance.

The *plasma before disruption* is carrier of thermal (E_{th}) and magnetic energy, $E_{mag} = 0.5\, I_p^2\, \mu\, R\; ln(\frac{8R}{a\sqrt{k}} - 2 + \frac{l_i}{2})$ associated with its toroidal electric current. At the end of the current quench the pre-disruptive plasma energy can be found as thermal energy on the plasma facing components (conducted and convected, E_{con}, or deposited by radiation, E_{rad}), and as electromagnetic energy - i.e. current - in electric conductors (E_{em}) coupled by mutual induction to the plasma. During the whole disruption, auxiliary heating is on and keeps inputing energy (E_{in}) into the plasma.

The energy balance equation for the plasma can be written as:

$$\Delta E_{mag} + \Delta E_{th} + \Delta E_{in} = \Delta E_{con} + \Delta E_{rad} + \Delta E_{em} \tag{1}$$

The energy balance can be applied to any time interval during the discharge. The different terms of the above equation have been computed for a variety of discharges both in the steady state phase and in disruptions. As an example, we discuss here the energy balance of a disruption after density limit (shot n. 13540) for the thermal quench and current quench phases separately. Time traces of several plasma parameters during the disruption are shown in Fig. 2. The energy in the following table is expressed in MJ.

phase.	ΔE_{mag}	ΔE_{th}	ΔE_{in}	$\Delta E_{div} - \Delta E_{div_{rad}} = \Delta E_{con}$	ΔE_{rad}	ΔE_{em}
th. qu.	> 0	0.16	~ 0	< 0.15	0.13	~ 0
whole	$\simeq 1.0$	0.16	0.08	0.5-0.4 = 0.1	0.7	0.15

The term E_{con} is the difference between the energy observed on the divertor plates by the thermography (E_{div}) and the energy deposited on the divertor plates by radiation ($E_{div_{rad}}$) and calculated from the radiation profiles, reconstructed from the bolometer. The energy balance over the whole disruption is within 30 % of the original energy content correct.

Energy onto the lower divertor plates.

The amount of energy deposited onto the divertor plates may change from disruption to disruption. Therefore it is necessary to look at the statistical distribution of the power deposited onto divertor and its different parts. The database described above is used for this analysis.

The amount of energy deposited on the lower divertor during the whole disruption is in average 30 % (and can reach 45 %) of the total pre disruptive energy of the plasma ($E_{tot} = E_{th} + E_{mag}$). During the 4 ms centered about the thermal quench, the energy deposited on the lower divertor is in average 90 % (and can reach 200 %) of the thermal energy. This suggests that during this time already a fraction of the magnetic energy is dissipated.

A statistical evaluation of the amount of energy deposited onto the different parts of the divertor is reported in the following table for the discharges of the Divertor II-lyra configuration. For this purpose the divertor has been subdivided in 8 regions as shown in Fig. 3. The table reports the amount of energy deposited on the divertor plate during the whole disruption (E_{div}) and during the 4 ms about the thermal quench (E^{th}_{div}) relative to E_{tot} and ($E_{th} + 0.1E_{mag}$) respectively; σ is the standard deviation of the distribution of these quantities for 30 discharges. S_n is the area of each divertor region.

Region n.	1	2	3	4	5	6	7	8
$E_{div(n)}/E_{tot}$ %		4.0	1.4	3.6	4.4	2.1	4.8	6.6
σ		2.2	0.4	1.0	1.1	0.8	2.5	1.7
$E^{th.qu.}_{div(n)}/(E_{th} + 0.1E_{mag})$ %		10.0	2.2	4.6	5.3	2.6	10.6	8.8
σ		6.0	0.7	1.7	2.2	1.3	6.6	3.0
S_n (m^2)	2.13	1.29	0.69	0.90	1.15	0.97	1.79	2.22

The thermography measurements on region n. 1 are not correct and therefore disregarded. (In the whole paper $E_{div} = \sum_n E_{div(n)}$, where $E_{div(n)}$ is the energy deposited on the nth region and $E_{div(1)}$ is assumed equal to $E_{div(8)}$.) We conclude that the *strike point modules* (region n. 2 and 7) are more loaded than the other part of the divertor during the thermal quench and that the energy is more uniformly distributed during the current quench. These results are illustrated in Fig. 4, where the mean of the amount of energy per unit surface has been plotted in an histogram for the different divertor regions and disruption phases. Similar results are obtained for the divertor II-b.

Future work.

Further work of analysis is underway to determine: the influence (1) of the divertor geometry, (2) of the disruption type, (3) of plasma parameters on the power deposition pattern and (4) the limits of the accuracy of the energy and power balance due to the error bars on the measurements.

Acknowledgments. We acknowledge usefull discussions with A. Loarte and G. Federici.

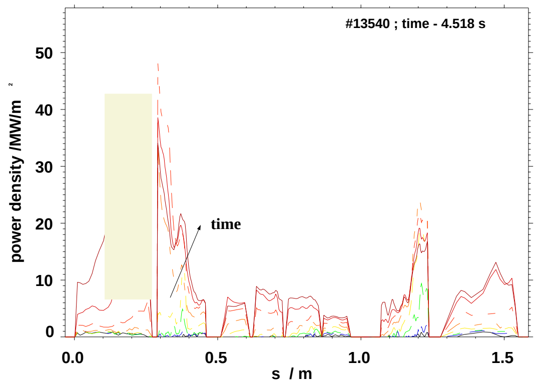

Figure 1. Time evolution of the power deposition profiles on the lower divertor plates during the thermal quench. The profiles are 0.12 ms apart.

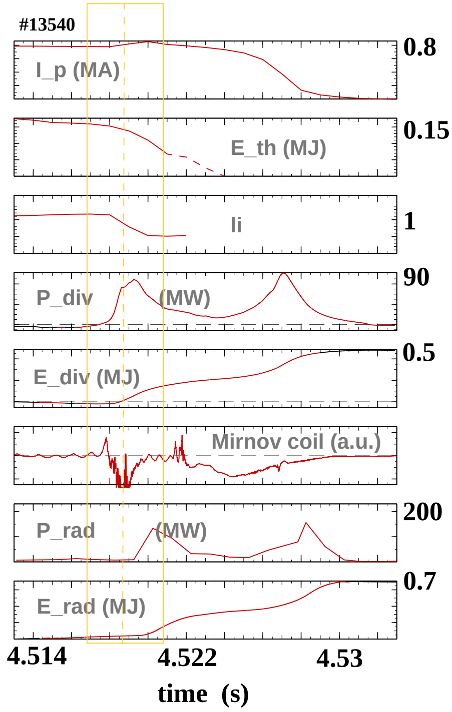

Figure 2. **(on the right)** Time histories of several plasma parameters during disruption. I_p is the plasma current, E_{th} is the thermal energy, li is the internal inductance, P_{div} and E_{div} are the power and energy deposited on the divertor plates, P_{rad} and E_{rad} are the power and energy radiated.

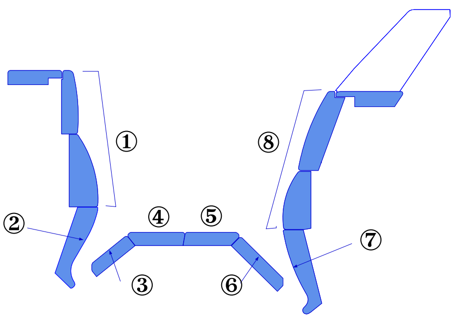

Figure 3. Divertor II-lyra geometry and its 8 regions.

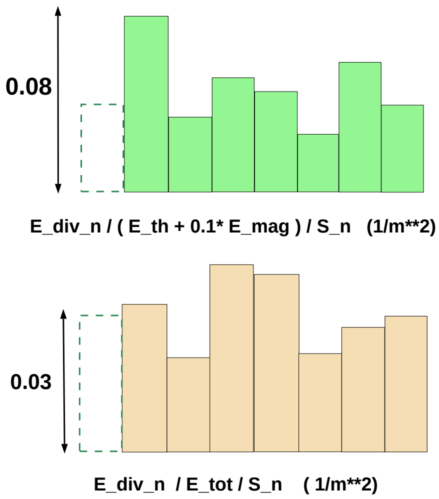

Figure 4. **(on the right)** Histogram of the energy per unit surface deposited on the different divertor regions (30 disruptions) during the thermal quench phase **(upper)** and whole disruption **(lower)**.

30th EPS Conference on Contr. Fusion and Plasma Phys.,
St. Petersburg, 7-11 July 2003 ECA Vol. 27A, P-1.135 (poster)

Max-Planck-Institut für Plasmaphysik, EURATOM Assoziation

Analysis of the power deposition in the ASDEX Upgrade divertor during disruptions

G. Pautasso, T. Eich, J.C. Fuchs, A. Herrmann, O. Gruber, A. Kallenbach and ASDEX Upgrade Group , MPI fuer Plasmaphysik, D-85748 Garching, Germany

INTRODUCTION

The power balance during disruptions in ASDEX Upgrade has been analyzed since the beginning of operation. The general picture of the power deposition mechanism in the Divertor I Phase (flat target plates) was as follows. The power density deposition profiles have always been so wide as to cover the whole divertor surface. During the thermal quench phase of the disruption up to 100 % of the thermal energy of the plasma was deposited onto the divertor plates within a few ms. In the successive current quench most of the magnetic energy associated with the plasma current was ohmically dissipated within the plasma and typically 30 % of it was found on the divertor plates. The majority of the disruptions in that experimental phase were density limits at relatively moderate plasma current (0.6-0.8 MA) and large q_{95} (4-6).

With the installation of the Divertor II-lyra and II-b and the exploration of new plasmas regimes (lower q_{95}, higher energy) the picture of power deposition has become more complex. In several discharges the thermal quench is relatively slow and the thermal energy starts leaking out of the plasma a few ms before the negative voltage spike. The power deposition profiles have remained very wide, spreading on the whole divertor surface and also outside of it.

Aim of this work is to check the power balance during recent disruptions and analyse the power deposition on the lower divertor plate from a statistical point of view.

DIAGNOSTICS

Radiation is measured by 100 bolometers, mounted in 7 cameras around the plasma. They allow the reconstruction of the radiated power profile. Time resolution: 1 ms.

Two IR cameras (in sec. 9 und 16) measure the photon emission from the lower divertor plates. Power deposition profiles may be inferred from the raw data.

Time resolution: 0.12-1 ms.
Spatial resolution: 1-2 mm.

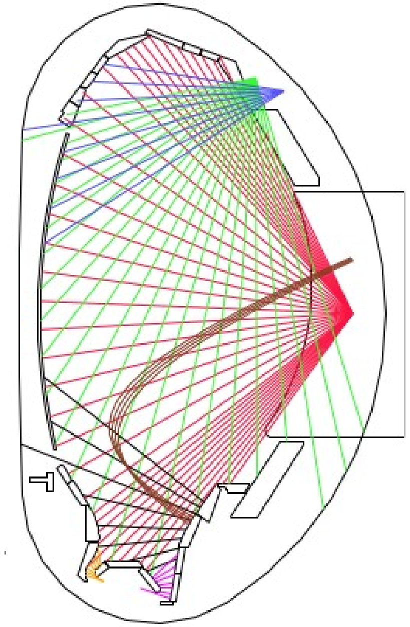

BOLOMETERS

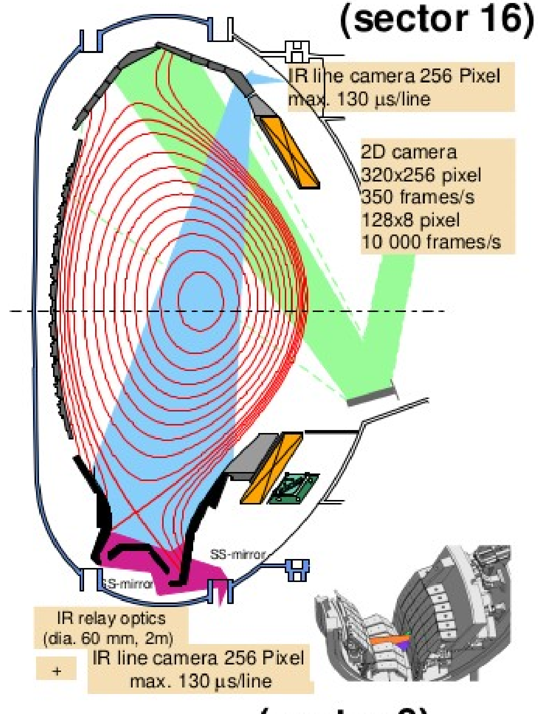

DIVERTOR GEOMETRY

The power deposition on the lower divertor (Div. II-lyra and Div. II-b) is analyzed in this work.
Data collected with the new IR camera looking at the inner wall and upper divertor are not reported here yet.

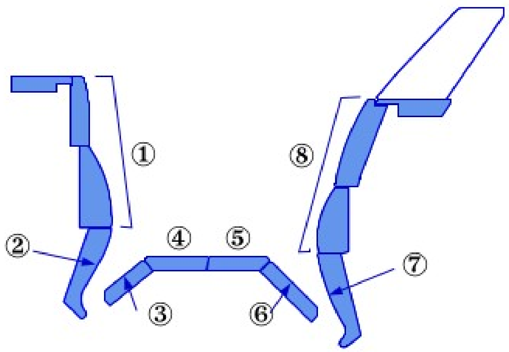

Divertor II-lyra

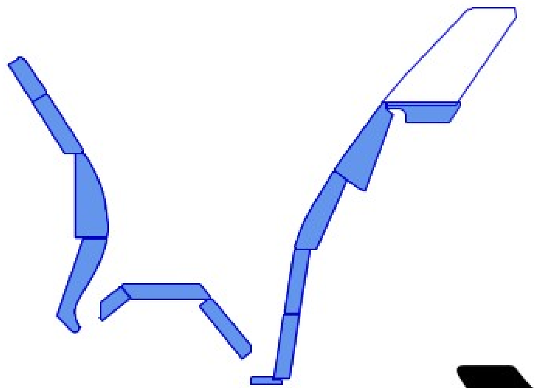

Divertor II-b

DATABASE

shot range: 13000-17500 (Jan. 2000 - Mai.2003)

Divertor II-lyra configuration: 30 discharges
(shot # < 14200)

Divertor II-b configuration: 14 discharges
(shot # > 14200)

Parameters:

plasma current (I_p) = 0.6 - 1 MA

q_95 = 2.5 - 6

thermal energy (E_th) = 50 - 500 kJ

magnetic energy (E_mag) = 0.7 - 1.8 MJ

disruption duration = 10 - 30 ms

Different causes, not yet analyzed

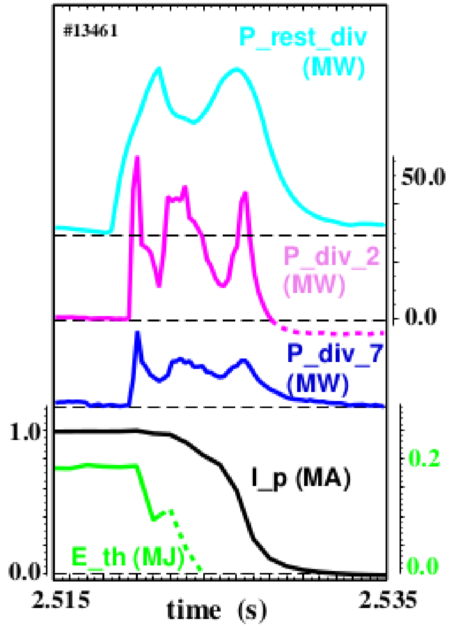

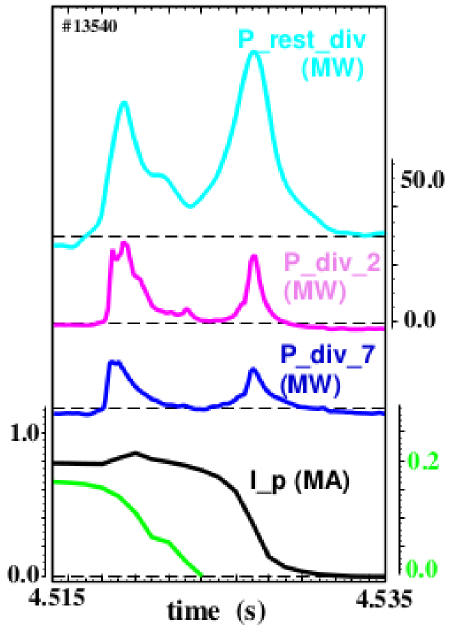

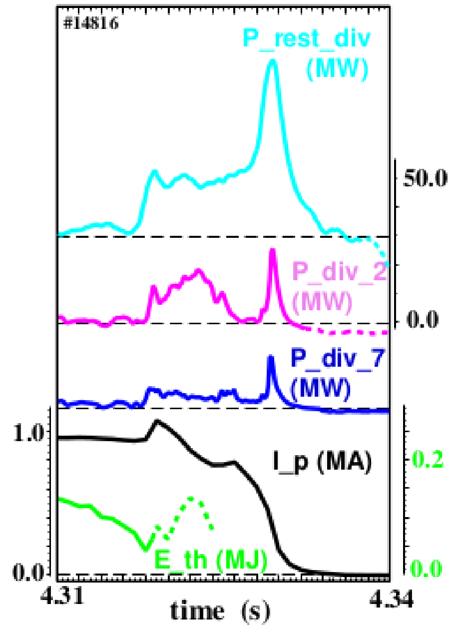

The power deposition on the divertor plates during the thermal quench lasts 2-3 ms.

There is no one typical time history of the power deposition during disruption but a variety of them.

ENERGY BALANCE

$$\Delta E\_mag + \Delta E\_th + \Delta E\_in = \Delta E\_rad + (\Delta E\_div - \Delta E\_div\_rad) + \Delta E\_em$$

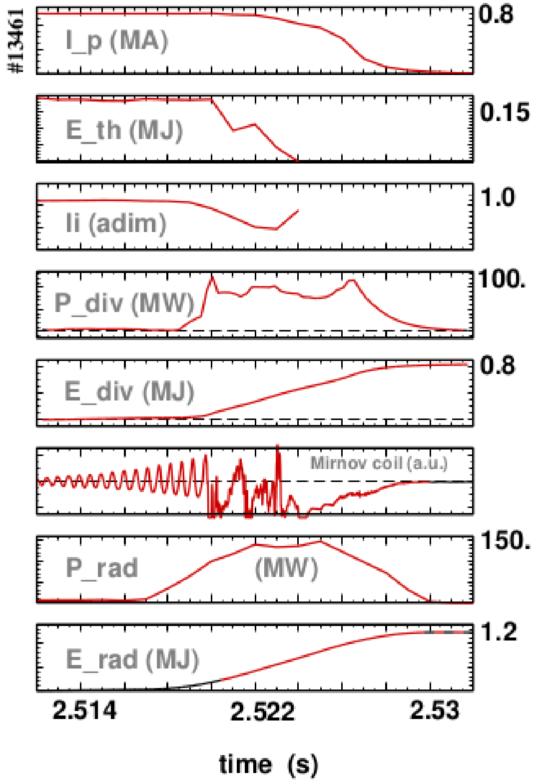

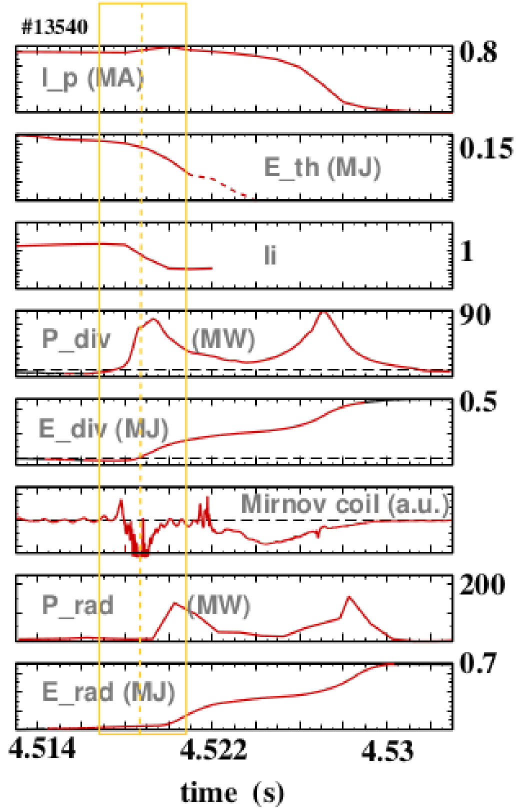

Energy balance in the ❶ thermal quench and ❷ overall

(MJ)	ΔE_mag +	ΔE_th ≈	ΔE_con +	ΔE_rad +	ΔE_struc
❶	> 0	0.19	< 0.25	0.16	~ 0
❷	1.7	0.19	(0.8-0.5=0.3)	1.2	~ 0.15

Energy balance in the ❶ thermal quench and ❷ overall

(MJ)	ΔE_mag +	ΔE_th ≈	ΔE_con +	ΔE_rad +	ΔE_struc
❶	> 0	0.16	< 0.15	0.13	~ 0
❷	1.0	0.16	(0.5-0.4=0.1)	0.7	~ 0.15

ENERGY LOAD on DIVERTOR

❒ The amount of energy deposited on the divertor plates during the whole disruption is 30 % in average (up to 45 %).

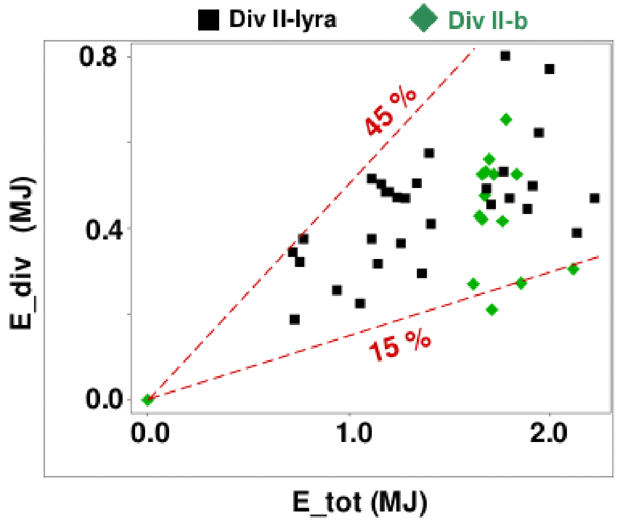

❒ During the 4 ms about the thermal quench E_div is:

① in average 90 % of pre-disruptive E_th.
➪ Part of the magnetic energy is already dissipated in this phase.

② in average 50 % of (E_th + 0.1 * E_mag).

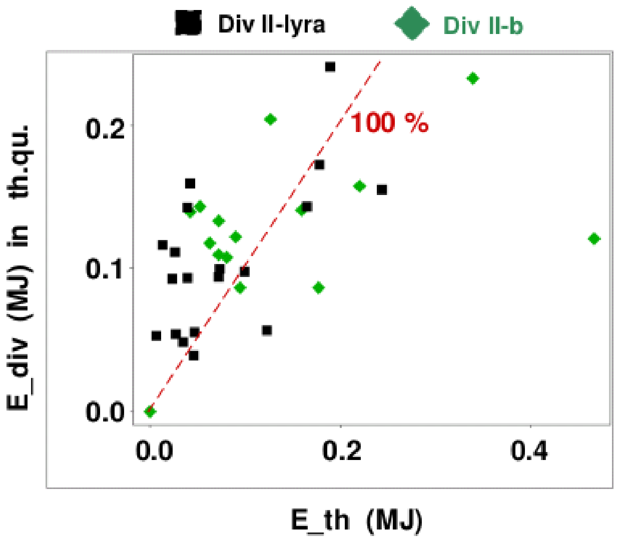

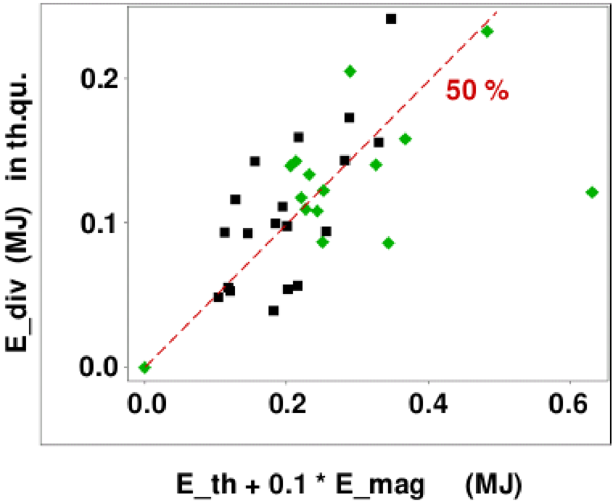

Langmuir probes measure strong ion flux during current quench

- largest ion fluxes on top end of divertor
- quiet phase in lower part of divertor between thermal and final quench
- strong ion fluxes during current quench suggest convective/conductive load

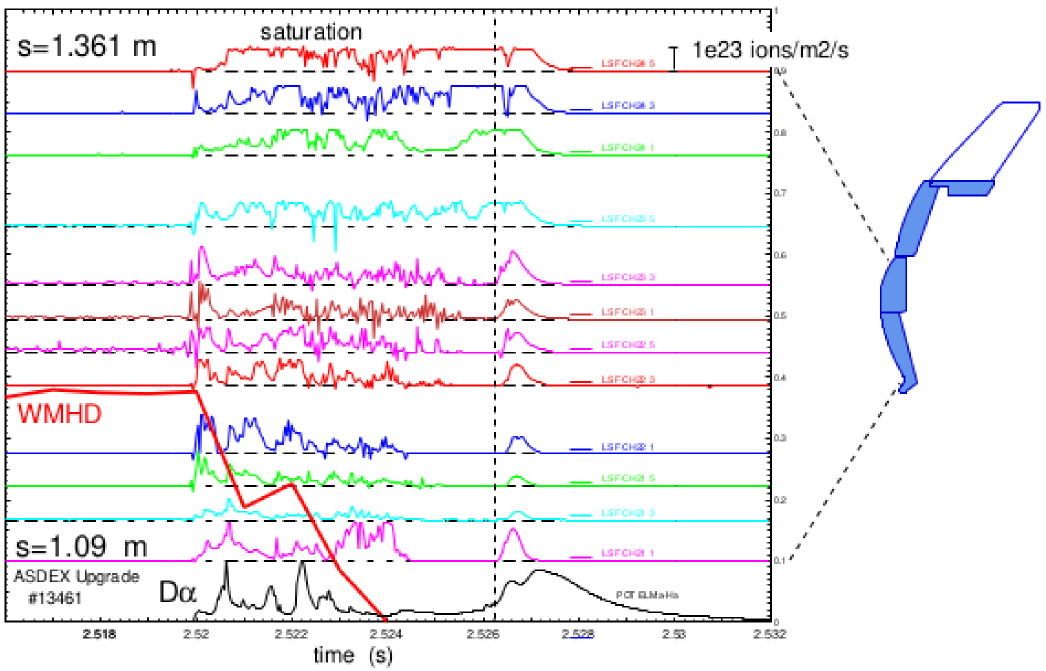

PROFILES OF POWER DENSITY

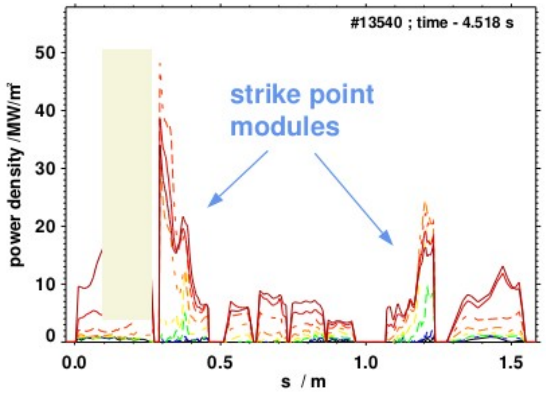

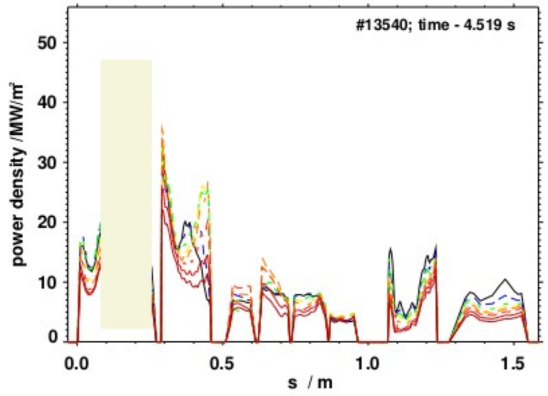

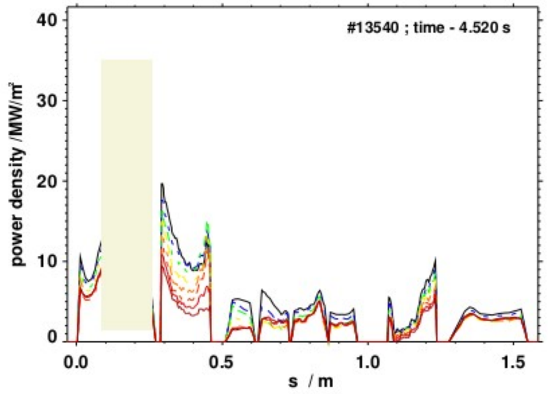

Thermal quench: Power density profiles on the lower divertor plate; Δt = 0.12 ms between profiles. Note the concentrated power load on the strike point modules on the top of a broad pedestal.

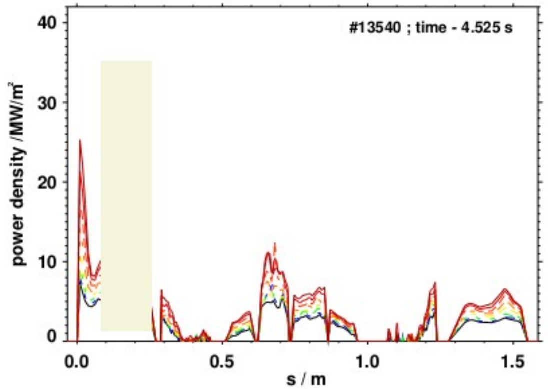

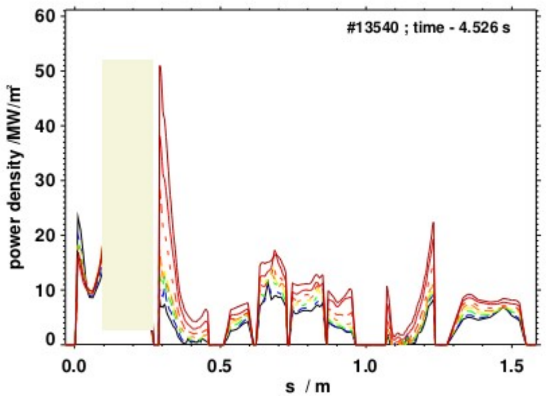

Current quench: unexpected concentration of power load on the strike point modules in this last phase of the disruption.

Halo currents

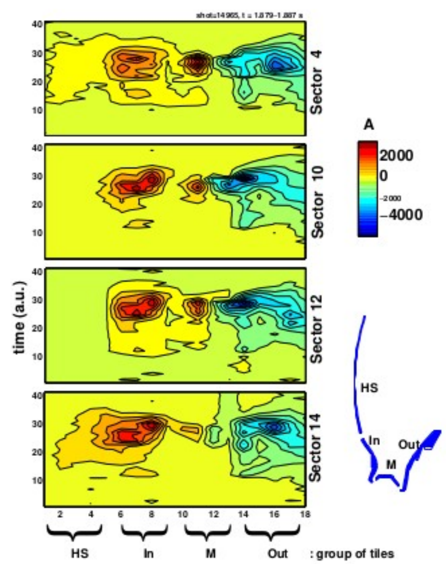

Contour plots of halo current: its footprint extends also outside of the divertor.

The thermography data are in the region not reliable.

Statistical distribution of the energy load on the divertor

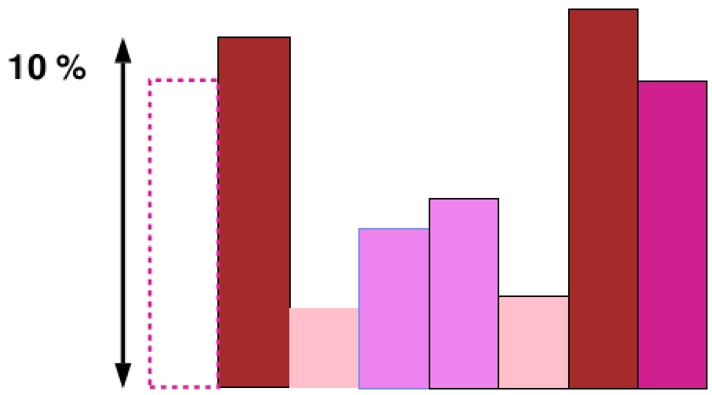

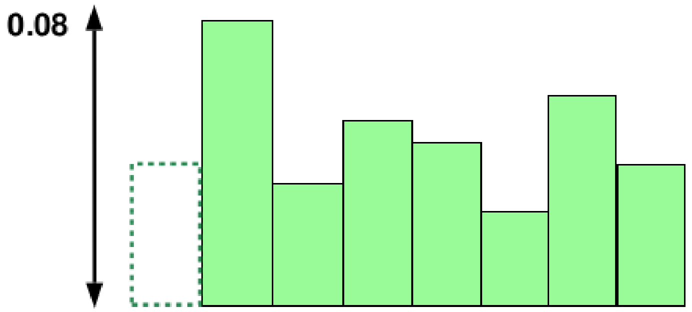

Histograms of the energy on the different regions of the lower divertor II-lyra during the thermal quench phase (above) and during the whole disruption (below) for the whole region (left) and per unit surface (right).
These are the mean values over 30 disruptions.

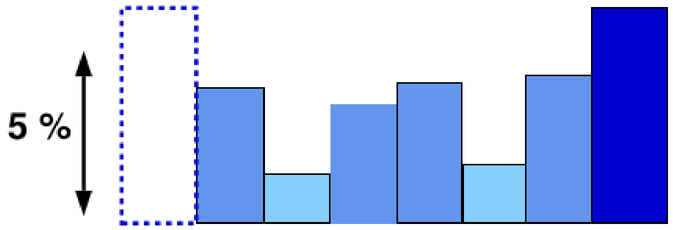

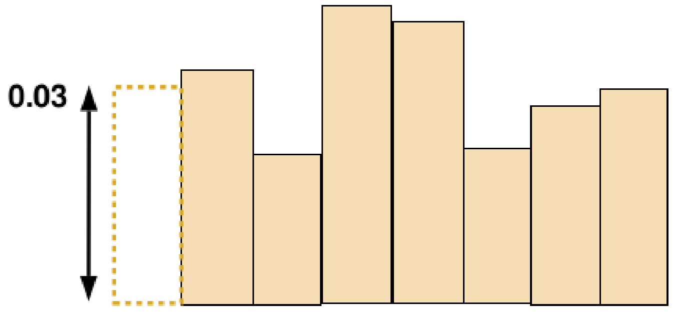

Radiated Power

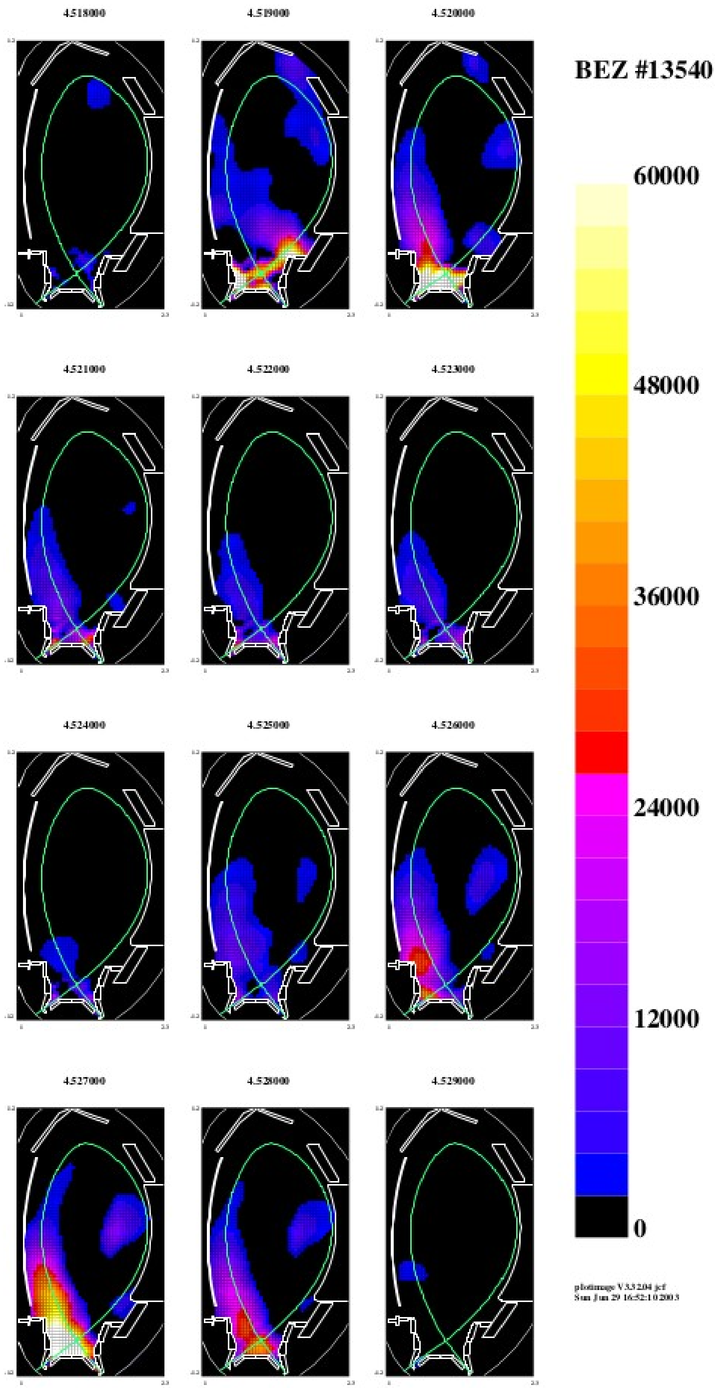

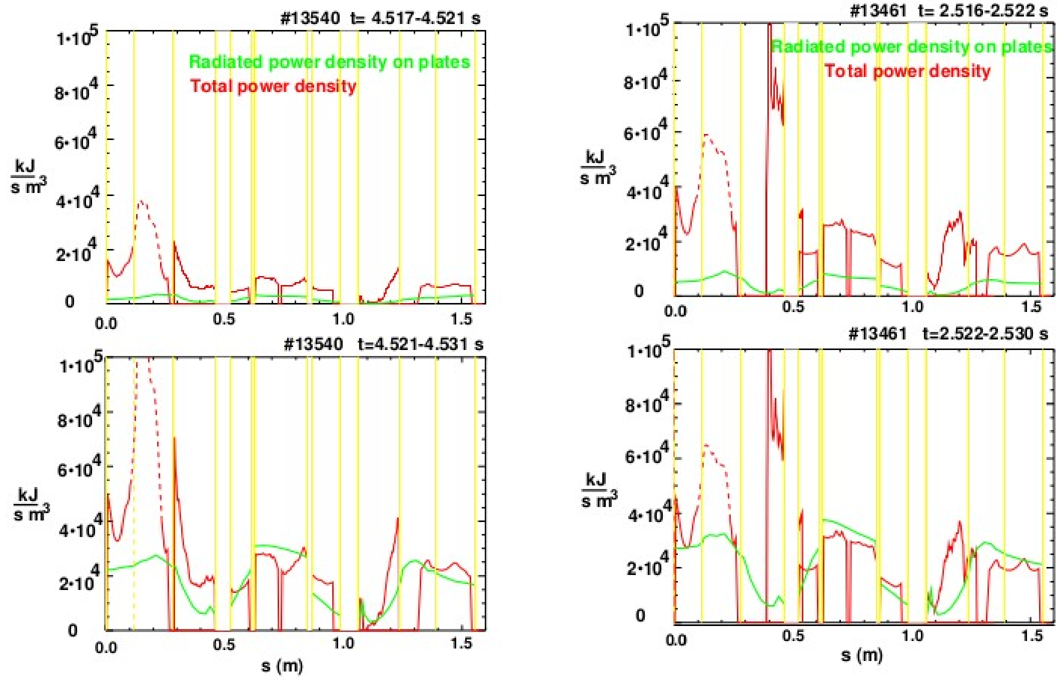

❒ The reconstruction of the radiated power profile is available for two discharges (at the moment).

❒ The 2D profiles of the radiated power (on the left; Δt=1 ms between frames) show that most of the power is radiated in the divertor region during both thermal and current quench phases.

❒ Most of the energy deposited on the divertor plates during thermal quench is conducted/convected.

❒ Most of the energy deposited on the divertor plates during current quench is radiated.

CONCLUSIONS and FUTURE WORK

❒ The time history of the power deposition on the lower divertor plate may change from shot to shot.

❒ The thermal quench phase lasts 2-3 ms .

❒ The power profile is broad and extends outside of the divertor plates.

❒ The energy balance is consistent within the uncertanties.

❒ An amount of energy equivalent and larger than the thermal energy of the pre-disruptive plasma is found on the divertor about the time of thermal quench. This energy is mostly deposited by convection and conduction.

❒ Up to 45 % of the total energy of the plasma is found on the divertor plates. Most of it is deposited as radiation.

❒ The divertor plates are rather uniformly loaded with power (on a time scale $\geq$ 4 ms).

❒ Future work should point out : (1) the influence of the divertor geometry, (2) of the disruption type and (3) of the plasma parameters on the power density distribution; (4) the limits of the accuracy of energy and power balance posed by the error bars of the measurements.

Details of power deposition in the thermal quench of ASDEX Upgrade disruptions.

G. Pautasso, T. Eich, A. Herrmann, D. Coster, C. Konz, O. Gruber, K. Lackner, W. Schneider and the ASDEX Upgrade Team, Max-Planck-Institut für Plasmaphysik, EURATOM Association, 85748 Garching, Germany

Introduction.

The issues of (1) duration of the thermal quench, (2) broadening of the SOL during thermal quench and (3) poloidal asymmetries of the conducted/convected heat fluxes in the SOL are presently subject of experimental investigation and analysis in ASDEX Upgrade. These parameters strongly influence the extrapolated thermal loads to the ITER first wall and the choice of the appropriate material. This work is part of the broader international effort aimed to review the Physics Basis for ITER on the basis of more recent experimental results.

The main diagnostics used for this work are the IR camera looking at the strike point modules of the lower divertor and the 2D IR camera monitoring the upper divertor or the inner and outer wall [1,2].

Duration of the thermal quench.

The duration of the thermal quench is predicted to be of the order of 1ms in ITER and assumed to scale proportionally to the minor radius of the device. The measurements of power deposition in divertor during thermal quench on ASDEX Upgrade show heat pulses longer than 1 ms and therefore do not support this assumption.

The duration of the thermal quench needs first of all to be defined empirically. It can be defined in several ways:

(1) as the decay time of the plasma thermal energy. This measurement is available from the equilibrium reconstruction with a time resolution as fine as 0.1 ms. Nevertheless the redistribution of the toroidal plasma current cause a large loop voltage that disturbs the magnetic measurements on which the FP reconstruction is based. Therefore the evaluation of the plasma thermal energy may not be valid during the thermal quench;

(2) as the decay time of the electron temperature. The ECE measurements are available with a fast time resolution (ms) but they are mostly in cut-off at the time of the disruption or may become affected by cut-off during the thermal quench. The extrapolation to ITER was based on ECE data [3];

(3) as the decay time of the SXR. The SXR emission is not measurable anymore during the last phase of the disruption or before the disruption itself because of the low plasma temperature;

(4) as the duration of the heat pulse on the divertor/wall.

In this work we base the definition of the thermal quench duration on the measurement of the heat pulse onto the divertor and in particular onto the strike point modules of the divertor. This restriction is necessary because the time history of the power varies from tile to tile in the poloidal direction.

Figure 1 shows a typical heat pulse integrated on the strike point modules of the lower divertor and the duration of the rising phase (τ_r, from $P = 0.15 * P_{max}$ to P_{max}; P is the deposited power) and the decay phase of the heat pulse (τ_d, from P_{max} to $0.5 * P_{max}$).

Only IR camera data sets with a time resolution (Δt_{therm}) of 0.12 and 0.24 ms have been used. The database for this work contains 50 shots, density and radiation limit disruptions, pertaining to the shot range 13000-15000. 35 % of data analyzed do not show an isolated peak, which falls in the definition of Fig. 1. For half of the remaining 33 cases, the heat pulse has a more complicated structure and results from the superimposition of several pulses. The remaining cases show a rising and a decaying phase, lasting a time τ_r and τ_d respectively, plotted in the histograms of Fig. 2. τ_r may be shorter than or as short as the time resolution of the thermography and up to 1-2 ms long. τ_d is longer than Δt_{therm}, in average 1 ms long, and therefore well resolved.

The attempt to characterize the time scale of the power deposition during thermal quench as function of plasma parameters is not very promising. τ_r and τ_d are not functions of the plasma thermal energy (in the 40-200 kJ range) and may vary within one order of magnitude. The dependence of τ_r and τ_d on the electron temperature (expected from theoretical considerations) cannot be assessed since measurements of electron temperature (from ECE) and density (from the DCN) are mostly not available before disruption.

Energy balance and reproducibility of the power deposition.

Recent dedicated experiments (shot range 18000-19000) aimed to measure the power deposition on the upper divertor in disruptions were carried out in Spring 2004 on ASDEX Upgrade. Density limit disruptions were caused by rising the density in a preprogrammed way with gas puffing. The plasma parameters were: upper single null, $I_p = 0.8$ MA, q_{95} = 3, 4.5 and P_{NI} = 2.5, 5 MW. The discharges with the lowest values of q_{95} and P_{NI} disrupted at E_{th} = 150 kJ. The other discharges underwent a series of minor disruptions, which degrades the energy from 150 to 40-50 kJ. The power deposition pattern is similar in these discharges. Nevertheless the fraction of thermal energy deposited on the primary divertor was striking different , ranging from 30 to 100 %. We do not have measurements of radiated power for this experiment. The causes of the energy *in-balance* may be different and cannot be quantitatively specified at the moment because of lack of diagnostic coverage:

(1) the power flux to the divertor is likely to be toroidally asymmetric (the IR measurements cover a thin poloidal profile of the divertor);

(2) the repartition between conducted/convected and radiated energy may differ from case to case;

(3) a fraction of the thermal energy may remain in the plasma.

Spatial distribution of the thermal energy deposited on the PFC during the thermal quench.

The ITER Physics Basis reports that the SOL width during the thermal quench broadens typically by a factor of 3 relative to the predisruption width. This prescription is not supported by recent and older measurements of ASDEX Upgrade which indicate that the SOL expands more than that during the thermal quench. Profiles of power deposition extend to the whole divertor and outside of it, as shown in Figure 3. Mapping of these profiles on the outer midplane show that the heat flux channel (expanded SOL) is larger than the sight of view of the IR camera (5 cm if mapped on the midplane). The typical

SOL width in ASDEX Upgrade is of the order of 1 cm .

For technical reasons the sight of view of a IR camera is limited to a fraction of the PFCs. Therefore a series of dedicated experiments is being carried out on ASDEX Upgrade using the 2D IR movable camera: the aim of the experiment is to measure the time history of the whole profile of deposited power by repeating the same disruption and taking snapshots of the wall with different IR views. The measurements show a rather homogeneous distribution of power on the inner wall and on the graphite coverage of the ICRH antenna on the outer wall. Already during preceding minor disruptions a few MW/m^2 are deposited on the inner and outer wall. During the thermal quench the power flux to the wall increases up to 5-10 MW/m^2 on most of the surface.

In-out asymmetry .

A common feature of power deposition in the analyzed thermal quenches is the time delay of 100 μs between the arrival of the heat pulse on the outer and the inner divertor plates. For the standard toroidal field (< 0) and plasma current (> 0) configuration the heat flux is firstly seen on the outer divertor plate in both of upper and lower X point configurations. The physical mechanism behind this observation is being investigated with the fluid neutral version of the SOLPS code [4].

The energy deposited in the thermal quench is predominantly deposited on the outer upper divertor. There is no evidence of significant poloidal asymmetry of the energy deposition on the lower divertor [5].

Comments and conclusions.

The heat flux onto PFCs during thermal quench mostly consists of overlapping pulses which prolong the duration of the thermal quench. The rising phase of the pulse may be shorter or as short as 100 μs; the pulse itself lasts longer than 1 ms.

The SOL width at the midplane during thermal quench is typically larger than 5 cm.

Significant distributed deposition of the energy on the inner and outer wall of the plasma chamber is observed during minor and major disruptions.

There are clear poloidal asymmetries in the energy deposition on the divertor with the upper outer plates being more loaded than the inner plate for plasmas with an upper single null configuration. We also observe a time delay between the arrival of the heat flux onto the outer and the inner divertor plates. The toroidal asymmetry of the heat deposition cannot be investigated at the moment because of lack of diagnostic coverage but it could be responsible for occasional energy in-balance during the thermal quench.

References.

[1] A. Herrmann et al., 16th International Conference on Plasma Surface Interactions, 5.2005, Portland, Main, USA

[2] T. Eich et al., 16th International Conference on Plasma Surface Interactions, 5.2005, Portland, Main, USA

[3] ITER Physics Basis Nuclear Fusion **39** (1999) 2137

[4] D. Coster et al., 19th IAEA Fusion Energy Conference, 10.1002, Lyon, France.

[5] G. Pautasso et al., 30th EPS Conference on Controlled Fusion and Plasma Physics, 7.2003, St. Petersburg, Russia

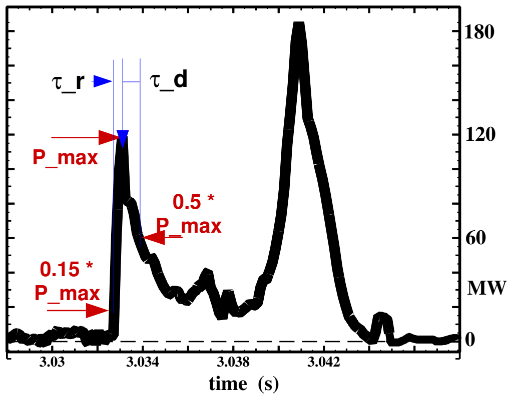

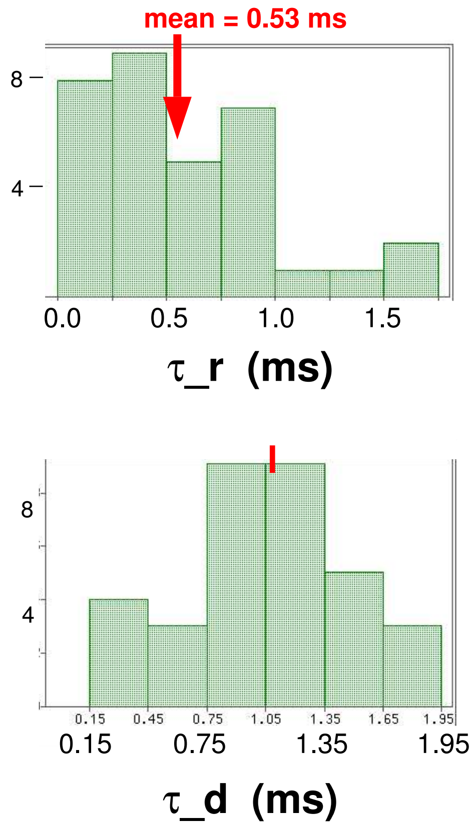

Figure 1. (top) Definition of the rising (τ_r) and decaying (τ_d) time of the power load on the divertor during thermal quench.

Figure 2 (right). Statistical distribution of τ_r and τ_d.

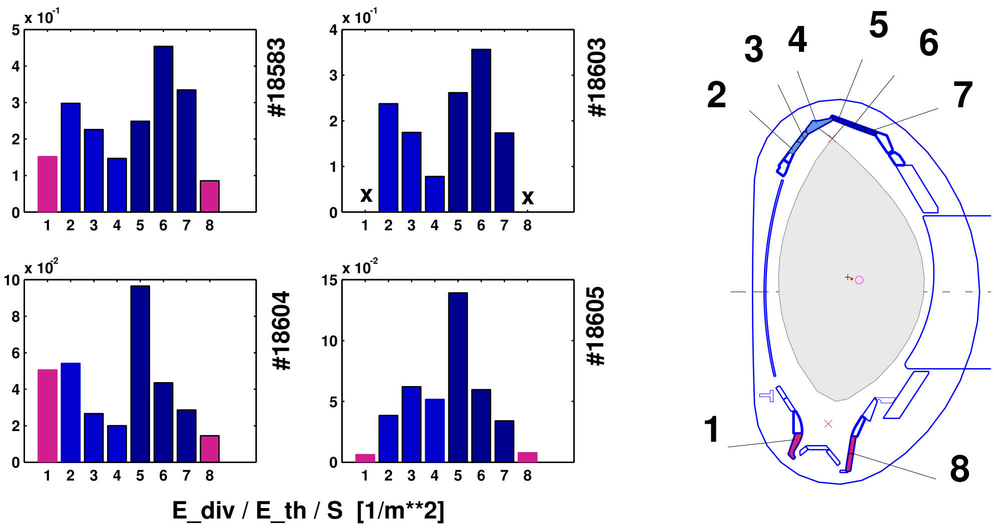

Figure 3. Distribution of the energy on different tiles of the divertor plates during the thermal quench for 4 density limit disruptions.

31st EPS Conference on Plasma Phys. London,
28 June - 2 July 2004 ECA Vol.28G, P-4.132 (poster)

Max-Planck-Institut für Plasmaphysik, EURATOM Assoziation

Details of power deposition in the thermal quench of ASDEX Upgrade disruptions

G. Pautasso, T. Eich, A. Herrmann, D. Coster, C. Konz, O. Gruber, K. Lackner, W. Schneider and ASDEX Upgrade Group, MPI fuer Plasmaphysik, D-85748 Garching, Germany

INTRODUCTION

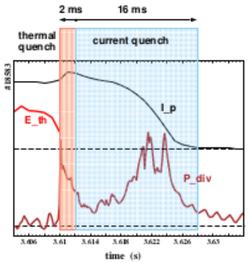

The issues of

(1) duration of the thermal quench,
(2) broadening of the SOL and
(3) poloidal asymmetries of the conducted/convected heat flux in the SOL during thermal quench

are presently subject of experimental investigation and analysis in ASDEX Upgrade. These parameters strongly influence the extrapolated thermal loads to the ITER first wall and choice of the appropriate material.

This work is part of the broader international effort aimed to review the Physics Basis for ITER on the basis of more recent experimental results.

DIAGNOSTICS

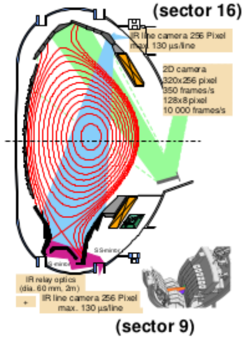

Two IR cameras (in sec. 9 und 16) measure the photon emission from the lower divertor plates. Power deposition profiles may be inferred from the raw data.
Time resolution: 0.12-1 ms.
Spatial resolution: 1-2 mm.

A 2D movable camera monitors the power deposition onto the upper divertor or inner/outer wall .

Time resolution > 0.1 ms
Spatial resolution: 1-2 mm

Duration of the thermal quench

The duration of the thermal quench is predicted to be ~ 1 ms in ITER and assumed to scale proportionally to the minor radius of the device. The measurements of power deposition during thermal quench in ASDEX Upgrade show heat pulses longer than 1 ms and therefore do not support this assumption.

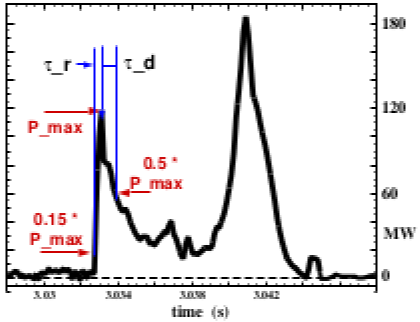

In this work we base the definition of the thermal quench duration on the measurement of the heat pulse on the strike point modules of the divertor. A rising (τ_r) and a decaying (τ_d) phase of the heat pulse are defined in the Figure above.

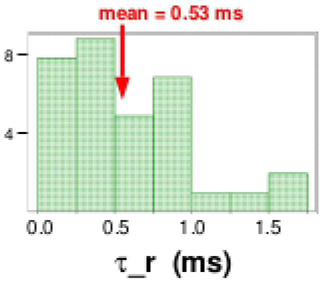

In the database of 50 disruptions, 35 % of the cases do not show an isolated peak.
For half of the remainig cases the heat pulse results from the superimposition of several pulses (shot 13647, on the right).

τ_r may be as short as the time resolution of the IR diagnostic and in average 0.5 ms .

τ_d is well resolved by the IR diagnostic and in average 1 ms long (histograms on the left)

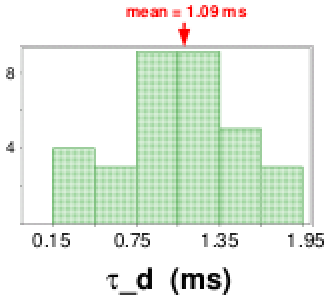

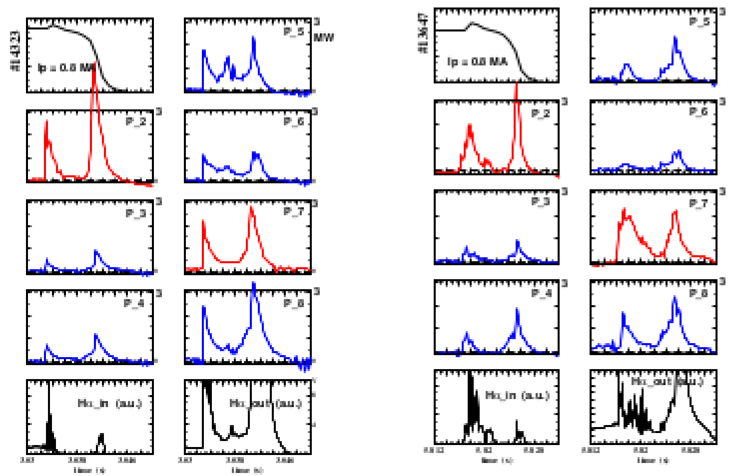

Reproducibility of power deposition

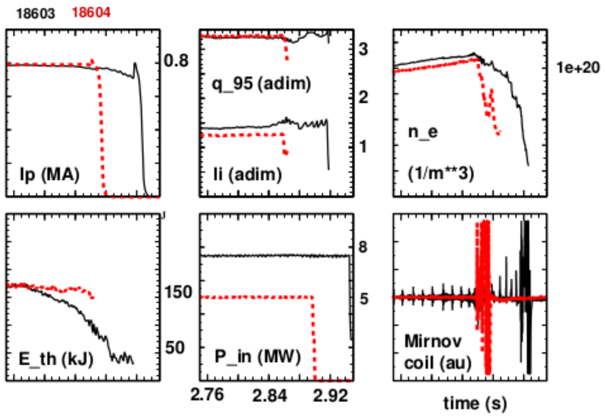

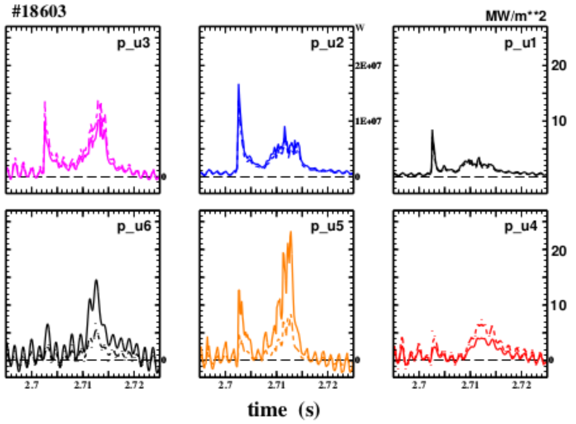

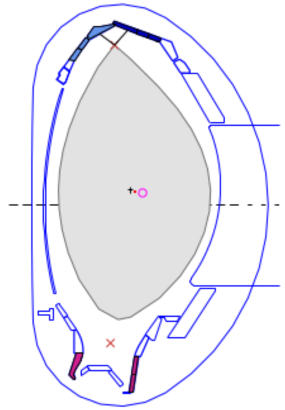

Density limit disruptions at similar plasma parameters were induced to study power deposition on the upper divertor (I_p= 0.8 MA, q_95= 3, 4.5, P_NI = 2.5, 5 MW).

Half of the discharges disrupted with E_th = 150 kJ, the other half with E_th= 40-50 kJ.

The power deposition pattern vary from discharge to discharge (histogram on the right).

The energy deposited onto the upper divertor plate during the thermal quench vary between 30 and 100 %.

The non-reproducibility of the measurements complicate the study of energy deposition.

The energy inbalance may be caused by the toroidal asymmetry of the deposition and by a different repartition between radiated and conducted/convected energy.

Spatial distribution of the energy deposition on the divertor plates during 3 ms about the thermal quench

Density limit disruptions, upper X point

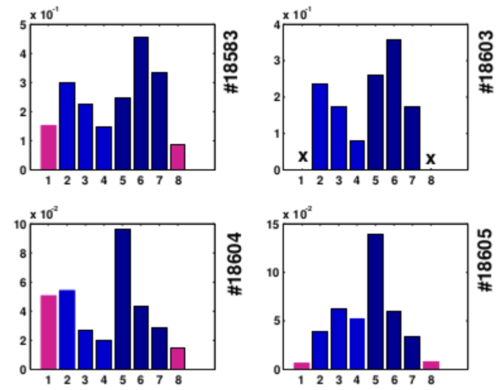

E_div / E_th / S [1/m**2]

Spatial distribution of the energy deposition

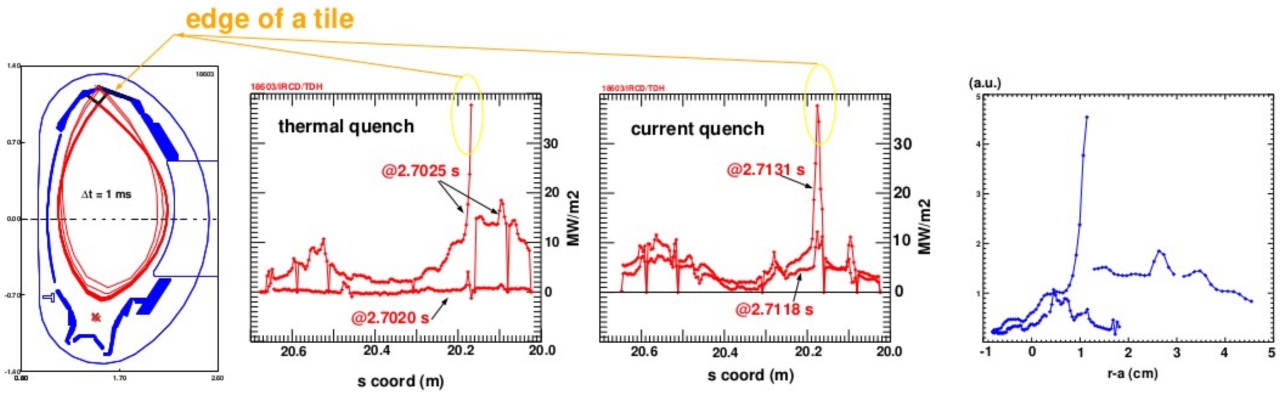

Profiles of power deposition extend to the whole divertor surface and outside of it both during the thermal and current quench .

The SOL expands beyond the sight of view of the IR camera (5 cm if mapped at the midplane).

Measurements of power deposition on the inner and outer wall show power fluxes up to a few MW/m^2 during minor disruptions and up to 5-10 MW/m^2 during the thermal quench on most of the surface (below). The plasma lost E_th = 150 kJ in both minor and major disruption.

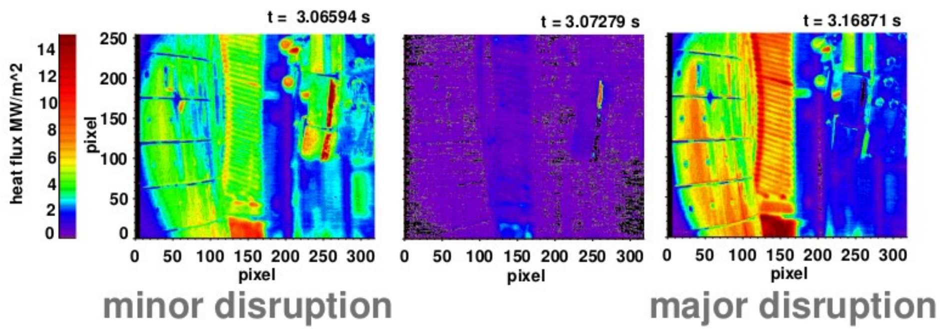

Simulation of the thermal quench

Some of the physical mechanisms which control the transfer of the energy from the plasma to the PFCs are investigated with the fluid neutral version of the SOLPS code.
A sudden increase of the thermal diffusion coefficient, which controls the radial transport, is imposed to simulate the thermal quench.
The dependence of the time and spatial evolution of the heat deposition on the PFCs as function of plasma parameter may then be studied.
Feathures seen experimentally are already found in the preliminar simulation of the phenomenon:

(1) the time delay between the arrival of the power pulse onto the outer and inner divertor seen in the measurements (Fig. 1) is also predicted by the code (Fig. 2) . The inner divertor is colder than the outer; conduction dominates at the outer divertor and is responsible for the faster process;

(2) the predicted temporal evolution of the pulse (Fig.3) has a form and duration similar to the observed one.

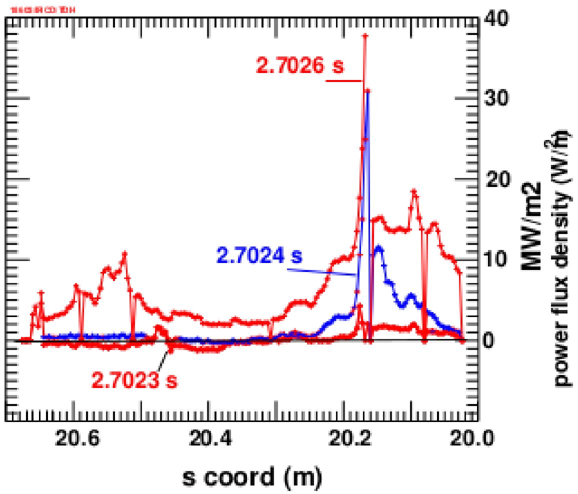

Fig. 1

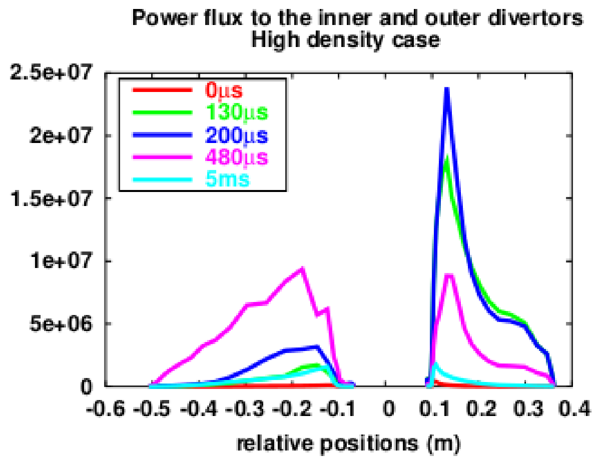

Fig. 2

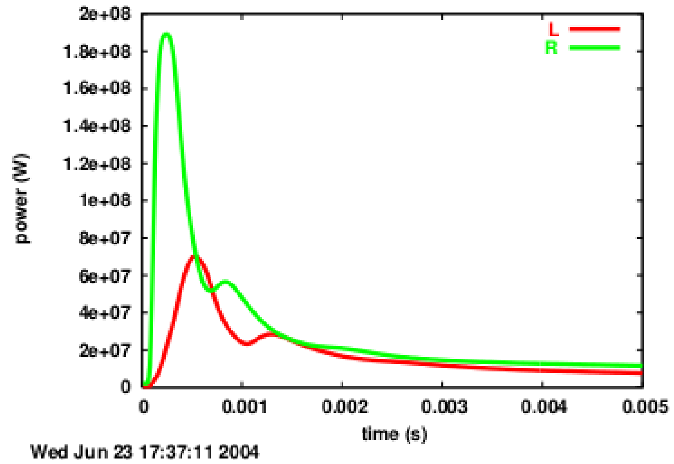

Fig. 3

CONCLUSIONS and FUTURE WORK

❑ The heat flux onto the divertor plates consists of overlapping pulses, which prolong the duration of the thermal quench. The rising phase of a single pulse may be shorter or as short as 100 μ. The pulse ityself lasts longer than 1 ms.

❑ The SOL width at the midplane during the thermal quench is larger than 5 cm.

❑ Heat fluxes comparable to the one observed on the divertor plates are observed on the inner and outer wall of the vessel during thermal quench.

❑ Poloidal asymmetries in the divertor and time delay between the arrival of the power flux to the outer and the inner divertor are experimentally observed.
Code simulations are carried out to understand these details on a physical basis.